Anomalous scaling of stochastic processes and the Moses effect

Lijian Chen,[1] Kevin E. Bassler,[1,2,3,*] Joseph L. McCauley,[1] and Gemunu H. Gunaratne[1,†]

[1]*Department of Physics, University of Houston, Houston, Texas 77204, USA*

[2]*Department of Mathematics, University of Houston, Houston, Texas 77204, USA*

[3]*Texas Center for Superconductivity, University of Houston, Houston, Texas 77204, USA*

(Received 30 January 2017; published 28 April 2017)

The state of a stochastic process evolving over a time t is typically assumed to lie on a normal distribution whose width scales like $t^{\frac{1}{2}}$. However, processes in which the probability distribution is not normal and the scaling exponent differs from $\frac{1}{2}$ are known. The search for possible origins of such "anomalous" scaling and approaches to quantify them are the motivations for the work reported here. In processes with *stationary increments*, where the stochastic process is time-independent, autocorrelations between increments and infinite variance of increments can cause anomalous scaling. These sources have been referred to as the Joseph effect and the Noah effect, respectively. If the increments are *nonstationary*, then scaling of increments with t can also lead to anomalous scaling, a mechanism we refer to as the Moses effect. Scaling exponents quantifying the three effects are defined and related to the Hurst exponent that characterizes the overall scaling of the stochastic process. Methods of time series analysis that enable accurate independent measurement of each exponent are presented. Simple stochastic processes are used to illustrate each effect. Intraday financial time series data are analyzed, revealing that their anomalous scaling is due only to the Moses effect. In the context of financial market data, we reiterate that the Joseph exponent, not the Hurst exponent, is the appropriate measure to test the efficient market hypothesis.

DOI: 10.1103/PhysRevE.95.042141

I. INTRODUCTION

A stochastic process is a sequence of random variables indexed either continuously or discretely, through a parameter often interpreted as time. Stochastic processes have been used to model a range of phenomena from stock prices [1–3] to precipitation levels [4–6] and animal locomotion [7–9]. A standard example is Brownian motion, which is described by the Wiener process $\mathcal{B}_t$. It has Gaussian distributed increments $\mathcal{B}_{t+\tau} - \mathcal{B}_t$ that are uncorrelated and independent of t. The probability distribution of $\mathcal{B}_t$ is also Gaussian, but with a width that grows as $t^{1/2}$. Thus, $\mathcal{B}_t$, also referred to as "normal" diffusive motion [10], is said to *scale* as $t^{\frac{1}{2}}$. More generally, processes are found that scale as t^H, where H is referred to as the self-affine exponent or the Hurst exponent [11].

Following experimental observations including those in biological systems [12], financial markets [3], and turbulence [13], it is of considerable interest to understand the nature of stochastic processes that scale anomalously. For example, $H \neq 1/2$ has been associated with the failure of the efficient market hypothesis (EMH) [14,15], namely that asset prices do not fully reflect all pertinent information on the market [16–18].

For processes whose increments lie on stationary, time-independent probability distributions, Mandelbrot identified two causes of anomalous scaling, which he referred to as the Noah effect and the Joseph effect, and furthermore he defined scaling exponents to characterize them [10,19,20]. The Noah effect represents the occurrence of large increments with anomalously large frequency resulting in a probability distribution with infinite variance. It is quantified by the latent exponent L; increment distributions with $L > 1/2$ have "fat tails" and exhibit anomalous scaling. The Joseph effect occurs when increments are correlated, and it is quantified by the Joseph exponent J. When $J \neq 1/2$, increment correlations can result in anomalous scaling. Mandelbrot's nomenclature is composed of biblical references: Noah built an ark to save mankind and other creatures from the great flood [21], an occurrence of an anomalously large event, and Joseph, interpreting a dream of Pharaoh's, counseled him concerning what he predicted would be a correlated sequence of years of abundance, followed by years of famine [22].

In this paper, we extend the characterization of scaling of stochastic processes to include those with nonstationary increments. Such processes can model the intraday prices of financial markets [23–25], daily precipitation levels [5,26–29], the abundance of solar flares [5,29–31], and temperature fluctuations in turbulence [5,13,29]. An additional mechanism that can produce anomalous scaling is identified. It is referred to as the Moses effect and characterized by the Moses exponent M, which quantifies the growth of the increment distribution. The nomenclature continues Mandlebrot's tradition: Moses led the Israelites after their Exodus from Egypt as they wandered through the wilderness having no stationary settlements [32].

We will generalize the definitions of H, L, and J and show that the sum of increments scales as t^H, with $H = L + J + M - 1$. For normal diffusive processes with stationary increments, $L = J = M = 1/2$ and thus $H = 1/2$. Anomalous scaling can occur when any of the exponents L, J, or M differs from $1/2$. We argue the even for processes with a Moses effect, as we have previously discussed [33], the EMH should be validated by measuring the Joseph exponent J, not the Hurst exponent H, since the EMH relates to the absence of correlations in market returns. A measurement of $J \neq 1/2$, indicating the presence of the Joseph effect, would violate the EMH, but anomalous scaling resulting from a combination of Noah or Moses effects can still be consistent with the EMH.

*bassler@uh.edu

†gemunu@uh.edu

The principal result of the work is the decomposition of the overall scaling H of the probability distributions into Joseph, Noah, and Moses effects via $H = J + L + M - 1$. Accurate numerical methods for establishing the four scaling exponents independently will be presented. They account for finite-time corrections to the scaling behavior, and they will be applied to standard and scaled versions of example stochastic processes to highlight the roles played by H, L, J, and M. Finally, exponents for a model of intraday trading in financial markets, i.e., variable diffusion processes [23,33–40], will be computed and compared to the results with an empirical analysis of financial market data.

The paper is organized as follows. Definitions of the scaling exponents and methods to quantify them are given in Sec. II. A collection of example stochastic processes that will be studied and the numerical methods to simulate them are given in Sec. III. Section IV presents the analysis of scaling in the various processes, demonstrating how the different effects can combine to yield an overall anomalous scaling. The methods used to accurately measure scaling indices are also presented in this section. In Sec. V, empirical financial market data are analyzed and compared to that of variable diffusion processes. The results are discussed in Sec. VI.

II. SCALING IN STOCHASTIC PROCESSES

Consider a one-dimensional stochastic process $\{X_t; t \in \mathcal{T}\}$ in which the set $\mathcal{T}$ can either be a subset of the real numbers or a subset of the integers. If the increments of the process

$$\delta_t(\tau) = X_{t+\tau} - X_t \tag{1}$$

have a probability distribution that is independent of t, then the stochastic process is said to be a stationary increment process (SIP). If instead the probability distribution of $\delta_t(\tau)$ depends on t, the process is referred to as a nonstationary increment process (NIP). Statistical analyses of SIPs can be preformed on a single time series of data, as the time independence of the increments permits a statistical ensemble to be constructed by time translations of the starting point. Statistical analyses of NIPs, on the other hand, generally cannot be performed on a single time series, requiring instead an ensemble of time series. If, however, a NIP begins anew at certain times, such as after a triggering event, then corresponding time translations may be used to construct a statistical ensemble from a single time series [23,41,42]. However, this may only be possible if the time between renewals has a finite average [43], since, more generally, weak ergodicity breaking [44,45] may prevent time averages from being equated with ensemble averages in diffusive processes that scale anomalously.

The generalization of time-series analyses to include NIPs necessitates generalizing the definitions of indices used to characterize scaling in SIPs. Consider an ensemble of realizations of a stochastic process, $\mathcal{X} = \{X_t^{(p)},\ p = 1,2,\dots\}$, each of which starts at the origin, i.e., $X_0^{(p)} = 0$, and has increments $\delta_t^{(p)}(\tau)$. The increments are random variables with probability distributions that can depend on t, but they are the same for all realizations p. These realizations can either have continuous or discrete time, but for the purposes of analyzing the scaling of the process, assume that they are sampled at regular intervals of time τ, which can be taken to be unity. The sampled times are then $t = 1,2,3,\dots$. Then

$$X_t = \sum_{s=0}^{t-1} \delta_s, \tag{2}$$

where here and in what follows the p superscript is suppressed for simplicity and $\delta_t = \delta_t(1)$. Define also the following random variables: the sum of the absolute values of increments,

$$Y_t = \sum_{s=0}^{t-1} |\delta_s|, \tag{3}$$

and the sum of increment squares,

$$Z_t = \sum_{s=0}^{t-1} \delta_s^2. \tag{4}$$

Probability distributions of these variables and of X_t over the ensemble $\mathcal{X}$ will be used to characterize and quantify the scaling of NIPs. The definitions of the scaling exponents that follow, which involve ensemble averages, i.e., over p, become equivalent to standard definitions for processes with stationary increments.

A stochastic process X is *self-similar* if, for any $a > 0$, there exists an exponent $H \geqslant 0$ such that

$$X_{at} \overset{d}{=} a^H X_t, \tag{5}$$

where "$\overset{d}{=}$" represents equality "in distribution," and H quantifies the scaling of the overall process. Note that, in general, only the one-point probability distribution $W(X_t)$ scales in self-similar processes; higher-order, multipoint distributions do not necessarily scale. Operationally, scaling of a suitable "width" of the probability distribution of X_t can be used to estimate H,

$$w[X_t] \sim t^H. \tag{6}$$

In this paper, we use the difference of the 75th quantile and the 25th quantile of the ensemble probability distribution as the measure of this width. For SIPs, this definition of H becomes equivalent to Mandelbrot's [10,11,20] and can be estimated by a variety of means, including detrended fluctuation analysis [46]. Using the quantiles circumvents difficulties in cases in which moments of the probability distribution diverge.

Since X_t is the sum of increments [Eq. (2)], it follows from the central limit theorem (CLT) that if the increment probability distributions (a) are uncorrelated, (b) have finite variance, and (c) are identical, independent of time, then the process will scale "normally," with $H = \frac{1}{2}$. Anomalous scaling in stochastic processes ($H \neq \frac{1}{2}$) may originate from the failure of one or more of these conditions. Joseph, Noah, and Moses effects are associated with the failures of conditions (a), (b), and (c), respectively, which are analyzed in the following subsections.

A. Joseph effect

The Joseph effect is associated with the failure of condition (a), and it can be quantified through a variant of rescaled range statistics (R/S) [10,19,47–49]. Estimate the range R_t

and standard deviation S_t of a stochastic process as

$$R_t = \max_{1\leqslant s\leqslant t}\left[X_s - \frac{s}{t}X_t\right] - \min_{1\leqslant s\leqslant t}\left[X_s - \frac{s}{t}X_t\right],$$
$$S_t^2 = \frac{1}{t}Z_t - \left[\frac{1}{t}X_t\right]^2. \quad (7)$$

Then the ensemble averaged ratio of R_t and S_t scales as

$$E[R_t/S_t] \sim t^J, \quad (8)$$

where J is the Joseph exponent. Negatively dependent processes have $J \in (0,1/2)$, positively dependent processes have $J \in (1/2,1)$, and independent processes have $J = 1/2$.

B. Noah effect

The Noah effect refers to the failure of condition (b), and it is quantified by the latent exponent L [10,19,20]. Suppose the tails of the increment distributions decay as

$$\lim_{x\to\infty} \Pr(|\delta_t| > x) \sim x^{-\gamma}, \quad (9)$$

where $\gamma \in (0,\infty)$. Then $L(t) := \max(\frac{1}{2}, \frac{1}{\gamma})$. In this paper, we only consider processes for which L is independent of time. Note that CLT condition (b) fails when $L > \frac{1}{2}$, because the variance of δ_t is then infinite. If the increment distribution is Gaussian, log-normal, or is any distribution with $\gamma \geqslant 2$, then $L = \frac{1}{2}$. If instead the increment distribution has fat tails with $\gamma < 2$, then $L = \frac{1}{\gamma}$. We further limit our considerations to processes with $L < 1$, as otherwise the increment distributions have infinite mean [50].

For time-series analyses, a more convenient and stable way to estimate the latent exponent is from the scaling of the ensemble probability distribution of the sum of increment squares, which can be estimated by the scaling of the median of the probability distribution of Z_t,

$$m[Z_t] \sim t^{2L+2M-1}, \quad (10)$$

where M is the Moses exponent introduced below. A proof for Eq. (10) is given in the Supplemental Material [51].

C. Moses effect

We define the failure of condition (c) as the Moses effect. It occurs when the increment distribution is time-dependent. We consider processes with increment distributions whose mean absolute deviation scales as

$$E[|\delta_t - E(\delta_t)|] \sim t^{M-\frac{1}{2}}, \quad (11)$$

where, as before, E is the ensemble average. For SIPs, $M = \frac{1}{2}$, whereas for NIPs, $M \neq \frac{1}{2}$.

In time-series analyses, a convenient and more robust way to estimate the Moses exponent is from the scaling of the ensemble probability distribution of the sum of the absolute value of increments, which can be estimated by the scaling of the median of the probability distribution of Y_t,

$$m[Y_t] \sim t^{M+\frac{1}{2}}. \quad (12)$$

A proof for Eq. (12) and a discussion of the effects on changes in the measurement frequency are given in the Supplemental Material [51]. Typically, we find that varying the increment interval, τ in Eq. (1), does not affect the leading scaling behavior of Y_t.

The anomalous scaling of NIPs can arise due to a combination of all three effects listed above. Equations (6), (8), (10), and (12) provide independent estimates of the four exponents. However, they are related through

$$H = J + L + M - 1. \quad (13)$$

This scaling relation provides a useful independent check of the estimates of the four exponents.

III. EXAMPLES OF SELF-SIMILAR PROCESSES

In this section, several model stochastic processes are introduced that will be used to illustrate the relationship (13). However, we emphasize that the relationship is expected to be valid for other stochastic processes as well.

A. Processes with Gaussian increments

The classic example is Brownian motion (BM), which consist of a sequence of identical, independent Gaussian increments [52]. BM can be generalized by including (a) correlations between increments and (b) time-dependent increments. One way to include long-term correlations is through fractional Brownian motion (FBM), denoted $\mathcal{B}_t^{(J,\frac{1}{2})}$, and defined below. These "correlations" can be characterized by an index J, which, as shown below, is the Joseph exponent. As for time-dependent increments, we limit consideration to processes whose increments scale in time. As shown below, growth can be characterized by the Moses exponent M. A stochastic process consisting of correlated and scaled Gaussian increments is denoted $\mathcal{B}_t^{(J,M)}$. In this notation, Brownian motion $\mathcal{B}_t$ is denoted $\mathcal{B}_t^{(\frac{1}{2},\frac{1}{2})}$.

Fractional Brownian motions $\mathcal{B}_t^{(J,\frac{1}{2})}$ that scale in time have the form

$$\mathcal{B}_t^{(J,\frac{1}{2})} \propto \int_{-\infty}^{0}[(t-s)^{J-\frac{1}{2}} - (-s)^{J-\frac{1}{2}}]d\mathcal{B}_s + \int_0^t (t-s)^{J-\frac{1}{2}}d\mathcal{B}_s, \quad (14)$$

where the proportionality constant is $1/\Gamma(J+\frac{1}{2})$, and $d\mathcal{B}_s \equiv \mathcal{B}_{s+ds} - \mathcal{B}_s = \mathcal{B}_{ds}$. The Gaussian increments of FBM are correlated [53,54], and the scaling exponents are derived as follows:

(i) Using Donsker's theorem [55] and the continuous mapping theorem [56,57], Avram *et al.* proved that the index J is the Joseph exponent [48,53,54].

(ii) Since individual increments are Gaussian-distributed, $L = 1/2$.

(iii) Since FBM is a SIP, $M = \frac{1}{2}$.

(iv) To derive H, let $v = s/t$, then $ds = tdv$, $d\mathcal{B}_s \overset{d}{=} \mathcal{B}_{ds} \overset{d}{=} \mathcal{B}_{tdv} \overset{d}{=} t^{\frac{1}{2}}d\mathcal{B}_v$. Thus, $\mathcal{B}_t^{(J,\frac{1}{2})} = \int_{-\infty}^{t}(t-s)^{J-\frac{1}{2}}d\mathcal{B}_s \overset{d}{=}$

$\int_{-\infty}^{1}(1-v)^{J-\frac{1}{2}}t^{J-\frac{1}{2}}t^{\frac{1}{2}}d\mathcal{B}_v \overset{d}{=} t^J\int_{-\infty}^{1}(1-v)^{J-\frac{1}{2}}d\mathcal{B}_v \overset{d}{=} t^J\mathcal{B}_1^{(J,\frac{1}{2})}$. From definition (5), $H = J$.

Observe that $H = J + L + M - 1$.

A scaled FBM is an NIP, except when $M = \frac{1}{2}$, and it is defined as

$$\mathcal{B}_t^{(J,M)} = \int_0^t s^{M-\frac{1}{2}}d\mathcal{B}_s^{(J,\frac{1}{2})}, \tag{15}$$

where $d\mathcal{B}_s^{(J,\frac{1}{2})} = \mathcal{B}_{s+ds}^{(J,\frac{1}{2})} - \mathcal{B}_s^{(J,\frac{1}{2})}$. Since increments $d\mathcal{B}_t^{(J,M)} = t^{M-\frac{1}{2}}d\mathcal{B}_t^{(J,\frac{1}{2})}$ and FBM is a SIP, M is the Moses exponent of $\mathcal{B}_t^{(J,M)}$. Furthermore, since $\mathcal{B}_t^{(J,M)} = t^{M-\frac{1}{2}}\mathcal{B}_t^{(J,\frac{1}{2})} = t^{J+M-\frac{1}{2}}\mathcal{B}_1^{(J,\frac{1}{2})}$ [see (iv) above], the self-similarity exponent is $H = J + M - \frac{1}{2}$. Consequently, $H = J + L + M - 1$.

1. Generation of FBM and scaled FBM

There are several methods proposed to generate FBM. Three of them—the Hosking method [58], the Cholesky method [59,60], and the Davies-Harte method [61–63]—are exact. We used the Davies-Harte method, which requires $O(N \log N)$ operations, due to its computational efficiency. The algorithm is predicated on computing the square root of the covariance matrix using the circulant matrix and a fast Fourier transform instead of much slower lower-upper triangular decomposition [59,60].

B. Processes with Lévy increments

Independent and identically distributed increments in the classic Lévy motions can be characterized by a single index L [50], which, as shown below, turns out to be the latent index. As before, we can generalize the underlying process by including correlations and time-scaling of increments. The resulting process will be denoted $\mathcal{L}_t^{(J,L,M)}$.

Increments of the Lévy motion $\mathcal{L}_t^{(\frac{1}{2},L,\frac{1}{2})}$ are stochastic variates from a probability distribution whose characteristic function is [64–66]

$$E[\exp(i\theta\delta)] = \exp[-|\theta|^{(1/L)}]. \tag{16}$$

The scaling exponents for Lévy motions are evaluated as follows:

(i) It has been shown that $\mathcal{L}_t^{(\frac{1}{2},L,\frac{1}{2})}/t^L \overset{d}{=} \mathcal{L}_1^{(\frac{1}{2},L,\frac{1}{2})}$, where $t \geqslant 0$ [11,50]. Consequently, $R(t) \sim t^L$. For $L > \frac{1}{2}$, increments of LM have the property that $\Pr(|\delta_t| > x) \sim x^{-1/L}$, which implies that $\Pr(\delta_t^2 > x^2 = y) \sim x^{-1/L} = y^{-1/2L}$. Applying CLT for processes with infinite variance [64,65], we obtain that $Z(t) \sim t^{2L}$, $S(t) = \sqrt{Z(t)/t} \sim t^{L-1/2}$. Thus, $E[R(t)/S(t)] \sim t^{1/2}$, and $J = \frac{1}{2}$ [10].

(ii) Increments satisfy $\Pr(|\delta_t| > x) \sim x^{-1/L}$, implying that L is the latent exponent.

(iii) For δ_t with $L < 1$, the first-order moment is bounded; since LM is a SIP, we have $E[|\delta_t - E(\delta_t)|] \sim t^0$, therefore $M = \frac{1}{2}$.

(iv) $H = L$ [11,50].

Note that $H = L + J + M - 1$.

As with the Brownian case, correlations between the variates can be induced using the fractional Lévy motion (FLM) defined as

$$\mathcal{L}_t^{(J,L,\frac{1}{2})} \propto \int_{-\infty}^{0}[(t-s)^{J-\frac{1}{2}} - (-s)^{J-\frac{1}{2}}]d\mathcal{L}_s^{(\frac{1}{2},L,\frac{1}{2})} + \int_0^t (t-s)^{J-\frac{1}{2}}d\mathcal{L}_s^{(\frac{1}{2},L,\frac{1}{2})}, \tag{17}$$

where $d\mathcal{L}_s^{(\frac{1}{2},L,\frac{1}{2})} = \mathcal{L}_{s+ds}^{(\frac{1}{2},L,\frac{1}{2})} - \mathcal{L}_s^{(\frac{1}{2},L,\frac{1}{2})} = \mathcal{L}_{ds}^{(\frac{1}{2},L,\frac{1}{2})}$ and the proportionality constant is $1/\Gamma(J+\frac{1}{2})$. Only the exponents J and H of a FLM differ from those of the corresponding Lévy motion. The Joseph exponent cannot be defined using R/S statistics when $J < \frac{1}{2}$, since the process is nowhere bounded in that case [11,20,50]. Thus, we restrict consideration to $J \geqslant \frac{1}{2}$. Avram *et al.* proved that the index J here is a Joseph exponent [48,54].

To estimate H, setting $s = av$, Eq. (17) can be expressed as

$$\mathcal{L}_{at}^{(J,L,\frac{1}{2})} \overset{d}{\propto} \int_{-\infty}^{0}[(at-av)^{J-\frac{1}{2}} - (-av)^{J-\frac{1}{2}}]a^L d\mathcal{L}_v^{(\frac{1}{2},L,\frac{1}{2})} + \int_0^t (at-av)^{J-\frac{1}{2}}a^L d\mathcal{L}_v^{(\frac{1}{2},L,\frac{1}{2})},$$

where the proportionality constant is the same as before. It follows that $\mathcal{L}_{at}^{(J,L,\frac{1}{2})} \overset{d}{=} a^{J+L-\frac{1}{2}}\mathcal{L}_t^{(J,L,\frac{1}{2})}$, and hence that $H = J + L - \frac{1}{2}$.

Finally, time-dependent increments can be generated through scaled FLM, which is defined via

$$\mathcal{L}_t^{(J,L,M)} = \int_0^t s^{M-\frac{1}{2}}d\mathcal{L}_s^{(J,L,\frac{1}{2})},$$

where $d\mathcal{L}_s^{(J,L,\frac{1}{2})} = \mathcal{L}_{s+ds}^{(J,L,\frac{1}{2})} - \mathcal{L}_s^{(J,L,\frac{1}{2})}$. Only the values of M and H of a scaled FLM differ from the corresponding exponents of the associated FLM. Specifically, using a calculation similar to that of H for FBM, $\mathcal{L}_t^{(J,L,M)} \overset{d}{=} t^{J+L+M-1}\mathcal{L}_1^{(J,L,M)}$, thus $H = J + L + M - 1$.

1. Generation of Lévy-stable random variables

Let ϵ be a uniform random variate on $(-\frac{\pi}{2}, \frac{\pi}{2})$ and let a random variable Φ be exponential with mean 1. Assume ϵ and Φ to be independent. Then the random variable

$$\delta = \frac{\sin(\epsilon/L)}{(\cos\epsilon)^L}\left(\frac{\cos((L-1)\epsilon/L)}{\Phi}\right)^{(L-1)}$$

is known to be distributed as Eq. (16) [50,67].

The Davies-Harte method cannot be used to generate FLM variates since the associated correlation function does not exist. We used an approach introduced by Stoev and Wu [68,69] that takes advantage of the circulant matrix and the fast Fourier transform to generate FLM. It requires $O(N \log N)$ operations. However, the algorithm can only simulate FLM approximately.

C. Variable diffusion process

Processes with Gaussian or Lévy increments, discussed above, have one common characteristic, namely that the increments are from a stable process and independent of the stochastic variable X_t. In this subsection, we introduce a set

of diffusive processes whose increments depend on X_t as well. Variable diffusion processes (VDPs) were introduced as a model for intraday variations in financial markets [23,39,40]. Here $\{X_t, t \geqslant 0\}$ satisfies the stochastic differential equation: $dX_t = \sqrt{D[X_t,t]}d\mathcal{B}_t$, where $D(X_t,t)$ is the diffusion coefficient. If the probability distribution function $W(X_t)$ at time t is self-similar [as given by Eq. (5)],

$$W(X_t) = t^{-H}\mathcal{F}(u), \tag{18}$$

where the *scaling variable* is $u = X_t/t^H$. Variable diffusion processes exhibit many *stylized facts* (i.e., common statistical features) reported in financial markets [34].

For variable diffusion processes with finite variance, Eq. (18) shows that $E[X_t] \sim t^H$ and $E[X_t^2] \sim t^{2H}$, and hence that $\mathrm{var}[X_t] = t^{2H}\mathrm{var}[X_1]$. The self-similarity of the probability distribution implies further that the diffusion coefficient scales as [34]

$$D(X_t,t) = t^{2H-1}\mathcal{D}(u). \tag{19}$$

The probability distribution $W(X_t)$ satisfies the Fokker-Planck equation:

$$\frac{\partial}{\partial t}W(X_t) = \frac{1}{2}\frac{\partial^2}{\partial X^2}[D(X_t,t)W(X_t)]. \tag{20}$$

Using Eqs. (18) and (19), we obtain $2H[uf(u)]' + [D(u)f(u)]'' = 0$, whose solution is

$$\mathcal{F}(u) = \frac{C}{\mathcal{D}(u)}\exp\left(-2H\int\frac{udu}{\mathcal{D}(u)}\right). \tag{21}$$

As an example, if $\mathcal{D}(u)$ is constant D_0, $\mathcal{F}(u) = C_0\exp(-\frac{1}{2D_0}u^2)$. If $\mathcal{D}(u) = D_0(1+\epsilon|u|)$ and $D_0 = \frac{2H}{\epsilon^2}$, where ϵ is a constant, then $\mathcal{F}(u) = \frac{\epsilon}{2}\exp(-\epsilon|u|)$, which is the biexponential distribution. The corresponding variable diffusion process $\{X_H(t), t \geqslant 0\}$ is given by

$$X_t = \int_0^t s^{H-\frac{1}{2}}\sqrt{\frac{2H}{\epsilon^2}\left(1+\epsilon\left|\frac{X_s}{s^H}\right|\right)}d\mathcal{B}_s.$$

The associated exponents are as follows:

(i) Since VDP is a Markov process, $J = \frac{1}{2}$.

(ii) For VDP with finite variance, $L = \frac{1}{2}$.

(iii) $dX_t = \sqrt{D(X_t,t)}d\mathcal{B}_t = t^{H-\frac{1}{2}}\sqrt{\mathcal{D}(u)}d\mathcal{B}_t$, thus $M = H$.

(iv) Since $W(X_{at}) = a^H W(X_t)$, the Hurst exponent is H.

Once again, $H = J + L + M - 1$.

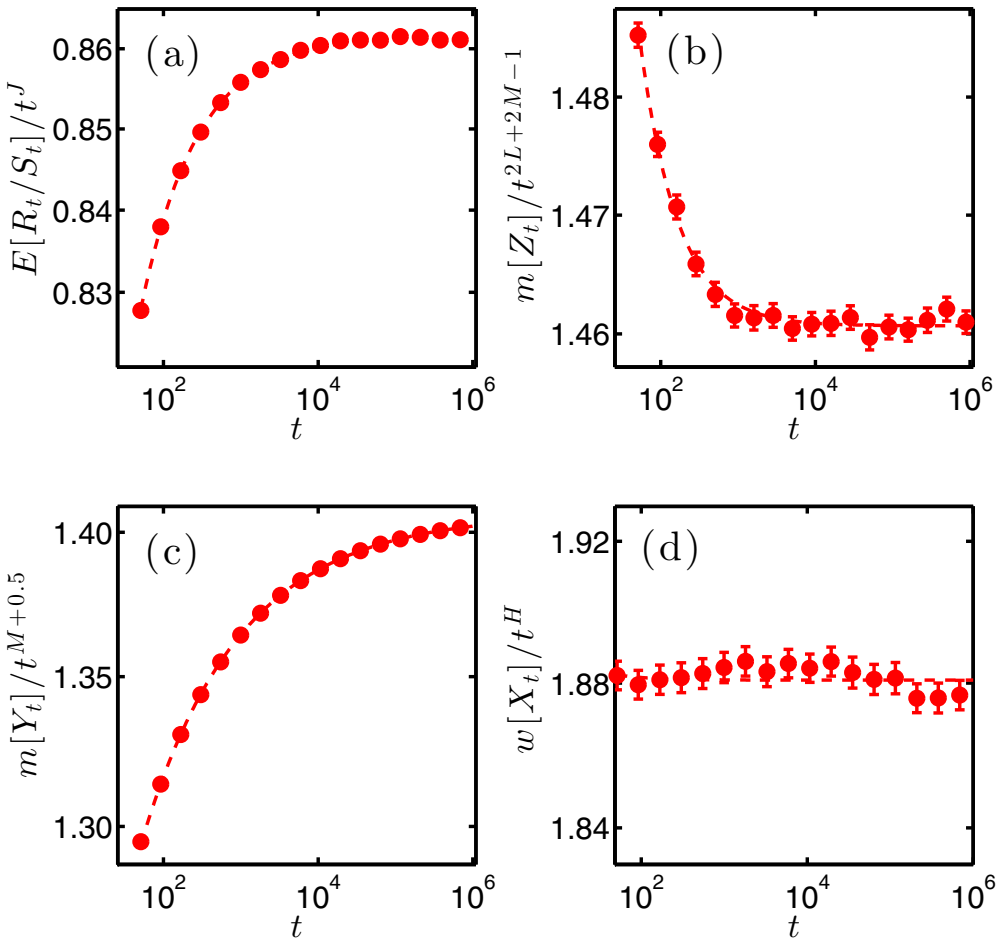

FIG. 1. Nonlinear fitting for SFLM ($J = 0.6$, $L = 0.6$, $M = 0.6$) using the form $y(t)/t^\Omega = a + bt^{-c}$ for finite-time corrections. (a) $y(t) = E[R_t/S_t]$, $\Omega = J$. (b) $y(t) = m[Z_t]$, $\Omega = 2L + 2M - 1$. (c) $y(t) = m[Y_t]$, $\Omega = M + 0.5$. (d) $y(t) = w[X_t]$, $\Omega = H$.

TABLE I. Estimates of the exponents for several classes of self-similar processes using the form $y(t) = at^{\Omega'} + bt^{\Omega'-c}$ for finite-time corrections. Note that when $J < \frac{1}{2}$, FLM cannot be evaluated using the R/S method [11].

Processes	J	L	M	$J+L+M-1$	H
BM	0.4997(5)	0.5000(1)	0.5000(1)	0.4997(5)	0.501(1)
SBM($M = 0.3$)	0.4996(5)	0.5000(1)	0.3000(1)	0.2996(5)	0.300(3)
SBM($M = 0.4$)	0.4999(5)	0.5000(1)	0.4000(1)	0.3999(5)	0.400(1)
SBM($M = 0.6$)	0.4995(4)	0.5000(1)	0.6000(1)	0.5995(5)	0.601(1)
SBM($M = 0.7$)	0.4993(4)	0.5000(1)	0.7000(1)	0.6993(5)	0.700(2)
LM($L = 0.71$)	0.4998(2)	0.7139(6)	0.5001(2)	0.7139(6)	0.714(2)
LM($L = 0.58$)	0.4996(3)	0.5883(2)	0.5000(1)	0.588(3)	0.588(3)
LM($L = 0.53$)	0.5004(4)	0.5266(2)	0.5000(1)	0.5270(5)	0.5256(9)
SLM($L = 0.53$, $M = 0.3$)	0.4998(3)	0.5268(3)	0.3000(1)	0.3266(6)	0.3254(4)
SLM($L = 0.53$, $M = 0.4$)	0.4999(7)	0.5263(2)	0.4000(1)	0.4263(9)	0.426(2)
SLM($L = 0.53$, $M = 0.6$)	0.4989(6)	0.5265(2)	0.6000(1)	0.6253(8)	0.626(2)
SLM($L = 0.53$, $M = 0.7$)	0.5000(4)	0.5265(2)	0.7000(1)	0.7265(5)	0.726(1)
SLM($L = 0.77$, $M = 0.3$)	0.5000(2)	0.769(5)	0.3004(4)	0.569(5)	0.569(1)
SLM($L = 0.77$, $M = 0.4$)	0.4998(2)	0.768(2)	0.4009(5)	0.669(2)	0.669(2)
SLM($L = 0.77$, $M = 0.6$)	0.5002(2)	0.769(5)	0.6006(5)	0.870(4)	0.869(2)
SLM($L = 0.77$, $M = 0.7$)	0.4997(2)	0.768(4)	0.7006(5)	0.969(3)	0.970(1)
FBM($J = 0.3$)	0.2994(5)	0.5000(1)	0.5000(1)	0.2994(5)	0.300(1)
FBM($J = 0.4$)	0.4000(5)	0.5000(1)	0.5000(1)	0.3999(5)	0.400(1)
FBM($J = 0.6$)	0.6001(3)	0.5000(1)	0.5000(1)	0.6001(3)	0.598(2)
FBM($J = 0.7$)	0.6998(2)	0.5000(1)	0.5000(1)	0.6998(2)	0.700(1)
SFBM($J = 0.3$, $M = 0.3$)	0.2988(7)	0.5000(1)	0.3000(1)	0.0988(8)	0.097(3)
SFBM($J = 0.3$, $M = 0.4$)	0.3004(5)	0.5000(1)	0.4000(1)	0.2004(5)	0.201(2)
SFBM($J = 0.3$, $M = 0.6$)	0.2997(5)	0.5000(1)	0.6000(1)	0.3998(6)	0.400(2)
SFBM($J = 0.3$, $M = 0.7$)	0.2989(6)	0.5000(1)	0.7000(1)	0.4989(6)	0.500(1)
SFBM($J = 0.4$, $M = 0.3$)	0.3990(6)	0.5000(1)	0.3000(1)	0.1990(6)	0.2007(5)
SFBM($J = 0.4$, $M = 0.4$)	0.3991(6)	0.5000(1)	0.4000(1)	0.2991(6)	0.3006(4)
SFBM($J = 0.4$, $M = 0.6$)	0.3993(4)	0.5000(1)	0.6000(1)	0.4993(4)	0.500(1)
SFBM($J = 0.4$, $M = 0.7$)	0.3994(4)	0.5000(1)	0.7000(1)	0.59994(4)	0.6001(5)
SFBM($J = 0.6$, $M = 0.3$)	0.5998(5)	0.5000(1)	0.3000(1)	0.3998(5)	0.4004(6)
SFBM($J = 0.6$, $M = 0.4$)	0.5998(3)	0.5000(1)	0.4000(1)	0.4998(3)	0.5004(5)
SFBM($J = 0.6$, $M = 0.6$)	0.5998(2)	0.5000(1)	0.6000(1)	0.6998(2)	0.700(1)
SFBM($J = 0.6$, $M = 0.7$)	0.6000(3)	0.5000(1)	0.7000(1)	0.8000(3)	0.800(2)
SFBM($J = 0.7$, $M = 0.3$)	0.6989(8)	0.5000(1)	0.3000(1)	0.4989(8)	0.498(2)
SFBM($J = 0.7$, $M = 0.4$)	0.6999(3)	0.5000(1)	0.4000(1)	0.5999(3)	0.5987(7)
SFBM($J = 0.7$, $M = 0.6$)	0.7000(2)	0.5000(1)	0.6000(1)	0.7999(2)	0.7997(4)
SFBM($J = 0.7$, $M = 0.7$)	0.6999(1)	0.5000(1)	0.7000(1)	0.8999(2)	0.900(2)
FLM($J = 0.4$, $L = 0.60$)	–	0.600(4)	0.4999(1)	–	0.4991(5)
FLM($J = 0.6$, $L = 0.60$)	0.5996(3)	0.600(3)	0.4999(1)	0.699(3)	0.699(1)
FLM($J = 0.4$, $L = 0.56$)	–	0.5560(3)	0.4999(1)	–	0.4564(7)
FLM($J = 0.6$, $L = 0.56$)	0.5996(3)	0.5558(4)	0.5000(1)	0.6553(7)	0.6547(4)
SFLM($J = 0.4$, $L = 0.60$, $M = 0.3$)	–	0.601(2)	0.2998(1)	–	0.300(1)
SFLM($J = 0.4$, $L = 0.60$, $M = 0.4$)	–	0.600(3)	0.4000(1)	–	0.401(3)
SFLM($J = 0.4$, $L = 0.60$, $M = 0.6$)	–	0.6003(4)	0.5999(1)	–	0.5995(4)
SFLM($J = 0.4$, $L = 0.60$, $M = 0.7$)	–	0.6002(4)	0.6999(1)	–	.6992(9)
SFLM($J = 0.6$, $L = 0.60$, $M = 0.3$)	0.5990(6)	0.602(3)	0.2998(2)	0.500(4)	0.499(1)
SFLM($J = 0.6$, $L = 0.60$, $M = 0.4$)	0.6000(2)	0.600(2)	0.4001(1)	0.600(2)	0.600(1)
SFLM($J = 0.6$, $L = 0.60$, $M = 0.6$)	0.5996(4)	0.6003(4)	0.5998(1)	0.7998(7)	0.798(1)
SFLM($J = 0.6$, $L = 0.60$, $M = 0.7$)	0.6000(3)	0.5993(8)	0.7001(1)	0.900(4)	0.898(1)
VDP($H = 0.3$)	0.4999(5)	0.498(4)	0.302(4)	0.300(5)	0.2996(7)
VDP($H = 0.4$)	0.4999(5)	0.500(3)	0.400(3)	0.400(4)	0.4003(5)
VDP($H = 0.6$)	0.4994(4)	0.500(2)	0.600(1)	0.599(2)	0.6008(4)
VDP($H = 0.7$)	0.4993(4)	0.499(5)	0.701(4)	0.699(5)	0.6999(7)

IV. RESULTS FROM SIMULATIONS

A. Finite-size corrections

Rescaled range statistics (R/S) analysis has been used extensively in studying persistence and long-term dependence in natural time series. The classical approach using the best linear relationship between $\log\{E[R/S(t)]\}$ and $\log(t)$ yields a biased estimate unless t is large [70–73]. Corresponding approaches to measure L, M, and H also suffer from analogous finite-time corrections. Reference [73] showed that the first-order finite-time corrections take the form

$$y(t)/t^{\Omega} = a + bt^{-c}, \tag{22}$$

where a,b,c are constants. As an example, Fig. 1 shows the nonlinear fit given by Eq. (22) for a SFLM with parameters $J = 0.6$, $L = 0.6$, and $M = 0.6$ for the (known) indices J, $2(L + M - \frac{1}{2})$, $M + \frac{1}{2}$, and H. Here, the reciprocal of the variance has been used as the weight of a point.

When exponents for a stochastic process are unknown (e.g., financial markets), we use the form

$$y(t) = at^{\Omega'} + bt^{\Omega'-c} \tag{23}$$

for finite-time corrections, and we estimate Ω' as well. For the remainder of the paper, we use this approach to estimate the exponents H, J, L, and M.

B. Exponents for different processes

For model stochastic processes, we use an ensemble of 100 000 stochastic realizations, each of length $t_{\max} = 1$ million. The lower cutoff is chosen to be $t_{\min} = 50$. We select $t_{\#} = 500$ points between $t_{\min}$ and $t_{\max}$; the ith point $t(i)$ ($i \in [1,2,\ldots,t_{\#}]$) is

$$t(i) = \text{round}\left[t_{\min}\left(\frac{t_{\max}}{t_{\min}}\right)^{\frac{i}{t_{\#}}}\right], \tag{24}$$

where round[x] represents the integer nearest to x; these points are (approximately) uniformly distributed in log scale. J, $L + M$, M, and H, estimated independently, are given in Table I. The reported standard errors are obtained through a bootstrap method. The relation $H = L + M + J - 1$ is found to hold for each process.

V. APPLICATION TO FINANCIAL MARKETS

A. Financial markets data

The data used for the analyses were 1-min valuations for the most actively traded exchange-traded funds (ETFs) in the U.S. market extracted from PiTrading.com. We restrict consideration to the most recent 2500 trading days (~10 y). Intraday trading is *assumed* to be a realization of the same stochastic process. The data provide open, close, high, and low prices within every minute; we use the close price for our analysis. Missing data, perhaps due to technical problems or errors, are replaced by the last recorded price. We studied the three most traded ETFs, namely the Dow Jones Industrial Average (DIA), the S&P 500 (SPY), and the PowerShare NASDAQ-100 (QQQ).

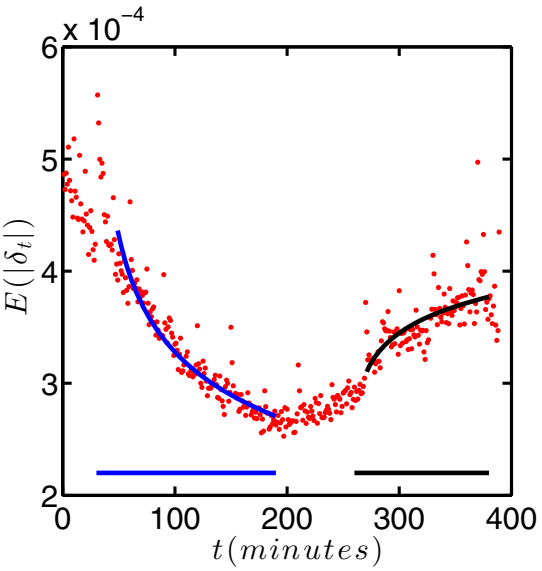

FIG. 2. Mean absolute value $E(|\delta_t|)$ of the increments of the SPY as a function of the time of day (beginning at 9:30 EST). Two scaling intervals where $E(|\delta_t|)$ can be fitted by power law $E(|\delta_t|) \sim t^{M-0.5}$, where t is measured from the start of each interval.

Stochastic processes underlying financial time series are represented using the *return*

$$X_t = \ln\frac{P_t}{P_0},$$

where P_t is the price of a financial asset at time t, and P_0 is a reference price, typically the price at the start of a session. The 1-min increments are

$$\delta_t = X_t - X_{t-1} = \ln\frac{P_t}{P_{t-1}}.$$

Note that $X_{t=0} = 0$, which is the necessary condition for X_t to scale, i.e., $X_t \overset{d}{=} t^H X_1$.

B. Scaling regions

1. Intraday seasonality

The analysis is predicated on the *assumption* that intraday variations of the return follow the same stochastic process each day. Consequently, return data from the 2500 trading days constitute the ensemble. To eliminate any drift within the trading day, the data are "detrended" by subtracting the ensemble average $E(\delta_t)$ at each t. The intraday pattern of $E(|\delta_t|)$ shows that the stochastic behavior is nonstationary within the day. $E(|\delta_t|)$ of SPY (as well as for the other ETFs) appears to scale as a power law within two intervals during the day, the first following the opening of the market and the second in the afternoon; see Fig. 2. The horizontal bars indicate the start and end of the two scaling intervals. The first ranges from 30 to 190 min and the second from 260 to 380 min from the start of the trading day.

C. Estimation of the exponents

The duration of the two scaling intervals is 160 and 120 min, respectively. The lower cutoff $t_{\min}$ for the finite-time

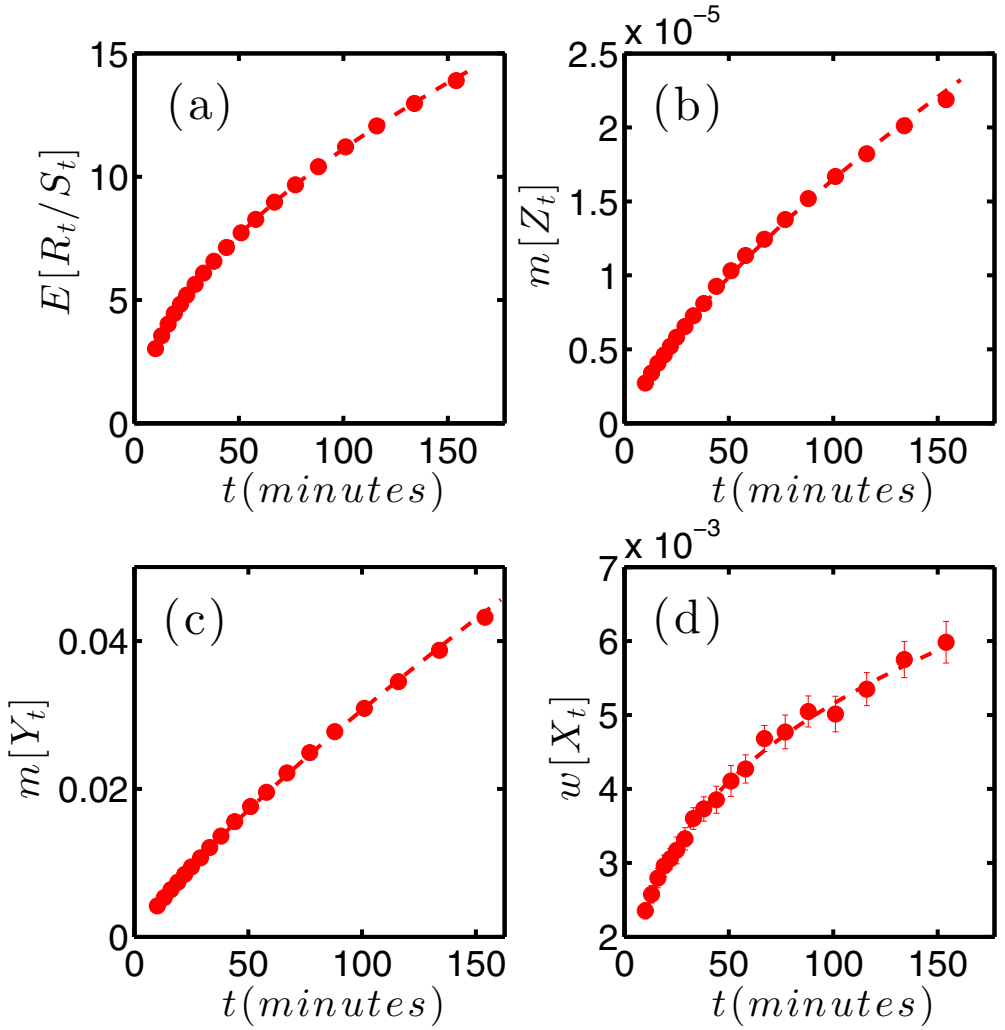

FIG. 3. Nonlinear fit for the S&P500 index SPY(30:190) using model $y(t) = at^{\Omega'} + bt^{\Omega'-c}$ for finite-time corrections. (a) $y(t) = E[R_t/S_t]$, $\Omega' = J = 0.500(2)$. (b) $y(t) = m[Z_t]$, $\Omega' = 2L + 2M - 1 = 0.587(4)$. (c) $y(t) = m[Y_t]$, $\Omega' = M + 0.5 = 0.790(2)$. (d) $y(t) = w[X_t]$, $\Omega' = H = 0.298(7)$. The error bars in (a), (b), and (c) are too small to be observed.

analysis (Sec. IV B) was set to 10 min. The total number of points used for the analysis, with intervals given by Eq. (24), is $t_\# = 60$. Methods outlined in the previous section were used for the analysis, and Fig. 3 shows the nonlinear fit for SPY(30:190). The indices extracted from the analyses are given in Table II, and conclusions include (i) $L \approx \frac{1}{2}$, implying that increments of the prices of ETFs are not from fat-tailed distributions, and (ii) $J \approx \frac{1}{2}$, implying the absence of long-term memory. The latter is validated using the autocorrelation function, which vanishes for time delays larger than 1 min. Furthermore, the relation $H = J + L + M - 1$ is validated.

The analyses outlined in Sec. IV were carried out for 100 000 ensembles of length 1 million. In contrast, financial

TABLE II. Estimates for the exponents for exchange traded funds using the form $y(t) = at^{\Omega'} + bt^{\Omega'-c}$ for finite-time corrections. SPY, DIA, and QQQ are abbreviations for the Standard and Poor 500 Index, the Dow Jones Industrial Average, and the PowerShare NASDAQ-100 Index, respectively.

Processes	J	L	M	$J + L + M - 1$	H
SPY(30:190)	0.500(2)	0.503(4)	0.290(2)	0.294(4)	0.298(7)
DIA(30:190)	0.502(2)	0.497(6)	0.287(4)	0.286(4)	0.29(1)
QQQ(30:190)	0.500(2)	0.501(6)	0.295(2)	0.296(5)	0.29(1)
SPY(260:380)	0.500(2)	0.511(9)	0.552(4)	0.564(7)	0.55(1)
DIA(260:380)	0.499(1)	0.50(1)	0.552(2)	0.56(1)	0.55(1)
QQQ(260:380)	0.501(1)	0.50(1)	0.550(4)	0.56(1)	0.55(1)

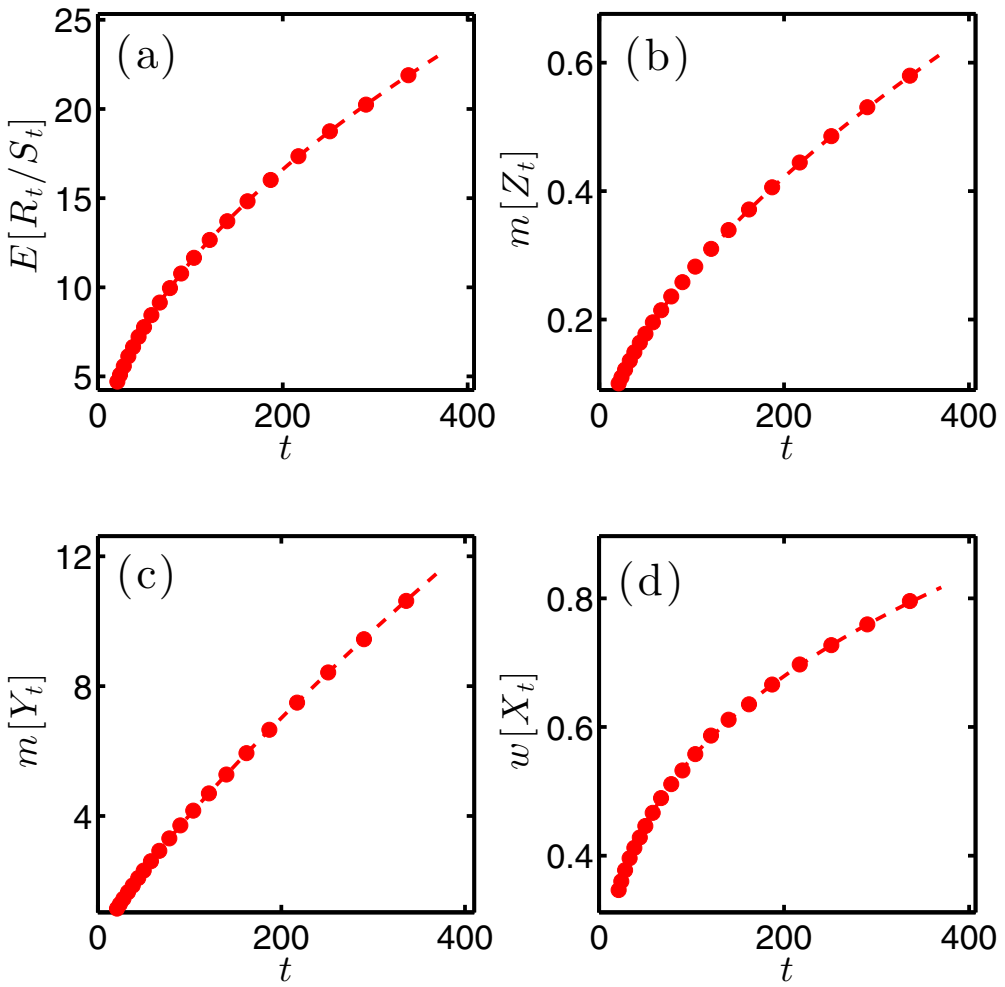

FIG. 4. Nonlinear fit for a variable diffusion process ($H = 0.3$) of length 370 using finite-time corrections of the form $y(t) = at^{\Omega'} + bt^{\Omega'-c}$. (a) $y(t) = E[R_t/S_t]$, $\Omega' = J = 0.499(3)$. (b) $y(t) = m[Z_t]$, $\Omega' = 2L + 2M - 1 = 0.596(4)$. (c) $y(t) = m[Z_t]$, $\Omega' = M + 0.5 = 0.8002(2)$. (d) $y(t) = w[Y_t]$, $\Omega' = H = 0.301(2)$. The errors bars are too small to be visible.

market analysis was conducted for an ensemble of size 2500, and the intervals were 160 and 120 min, respectively. One may inquire whether the information extracted from these short processes through finite-size corrections is reliable. To address this issue, we recomputed the indices for the variable diffusion process over a time interval $t_{\max}$. As described below, $t_{\max}$ is evaluated using the relaxation of the finite-time indices. Specifically, we write Eq. (22) as

$$E[R/S(t)] = at^J\left[1 - \left(\frac{t}{\tau}\right)^{-c}\right],$$

where $\tau = (-\frac{b}{a})^{\frac{1}{c}} = 0.18(1)$ is a time scale for convergence of the index. To estimate $t_{\max}$ for the VDP, we note that the nonlinear fit for J for SPY(30:190) gives $\tau = 0.42(5)$. The corresponding analysis of the VDP ($H = 0.3$) should be of length $t_{\max} = \frac{0.42}{0.18} \times 160 \approx 370$, $t_{\min} = \frac{0.42}{0.18} \times 10 \approx 20$. Figure 4 shows the nonlinear fit for this VDP with $t_{\max} = 370$. The estimated exponents are $J = 0.499(3)$, $L = 0.497(6)$, $M = 0.300(4)$, $J + L + M - 1 = 0.297(5)$, and $H = 301(2)$. We thus infer that exponents computed for financial markets are reliable.

VI. CONCLUSIONS

There are increasing numbers of examples, ranging from variations in biological systems [12] and thermal fluctuations in turbulence [13] to price variations in financial markets [3], where the probability distributions associated with a stochastic process exhibit anomalous scaling and are non-Gaussian. The anomalies can have different origins, and the goal of the work reported here is to disentangle them. Previous studies on stationary processes [10,20] had established that infinite variance of increments (the Noah effect) and long-time correlations between increments (the Joseph effect) are two sources of the anomaly. However, these studies failed to recognize that the time dependence of the increments themselves can also be a source of anomalous scaling. In this paper, we showed how scaling of the increments with time, referred to as the Moses effect, can also contribute to anomalous scaling. Noah, Joseph, and Moses effects, characterized by L, J, and M, respectively, are independent, and the overall scaling of the probability distributions, quantified by the Hurst exponent H, is given by $H = L + J + M - 1$. As was emphasized, definitions of the exponents require the use of an ensemble

of (nominally identical) stochastic trajectories when the underlying processes are time-dependent.

Numerical approaches of time-series analysis to accurately estimate each of the four scaling exponents independently were introduced. They are based on the use of medians and quantiles, which is especially appropriate for probability distributions lacking finite variance. These methods account for finite-time power-law corrections to scaling. The fact that the four indices can be measured independently allows the scaling relation that connects them to be verified, providing a stringent numerical check on the accuracy of the time-series analysis. The new numerical techniques were applied to a variety of different stochastic processes, including ones with both stationary and nonstationary increments, with and without long-time autocorrelations, and with both finite and infinite increment variance, to demonstrate the role of each effect toward anomalous scaling.

Financial time series of exchange-traded funds (ETFs) were analyzed as an application of the methods introduced here. As has been found to be the case for other financial markets [23,39,40], the intraday prices of ETFs can be considered to be governed by nonstationary stochastic processes that repeat each trading day. We find two intervals where the underlying stochastic process scales anomalously with $H \neq 1/2$, which is often associated with a violation of the efficient market hypothesis (EMH). However, we find that $L = 1/2$ and $J = 1/2$, i.e., neither the Noah effect nor the Joseph effect is observed in financial markets. The deviation from $H = 1/2$ results solely from the Moses effect ($M \neq 1/2$). Previously, it was proposed that the true test of the EMH should be the lack of correlations, i.e., $J = 1/2$, and not $H = 1/2$ [33]. Therefore, our analysis reiterates that ETF markets satisfy the EMH, despite the fact that they exhibit anomalous scaling. Finally, consistent with other recent studies of intraday trades in financial markets [23,33,42], we found that a variable diffusion process accurately models the scaling behavior in the two scaling intervals.

Although the scaling exponents defined here characterize the sources of anomalous scaling of the distribution functions, they do not uniquely identify higher-order statistics or the underlying stochastic processes themselves. As an example, a scaled Brownian process and a variable diffusion process can have the same exponents as the first stage of stock markets (i.e., with $J = \frac{1}{2}$, $H = \frac{1}{2}$, and $M = 0.3$). As discussed in the Supplemental Material [51], VDP exhibits volatility clustering (i.e., the absolute values and the squares of increments exhibit long-time correlations) while the corresponding scaled BM fails to do so. Volatility clustering is one of the well-known *stylized facts* on financial market dynamics [74].

It would be interesting to apply the methods of time-series analysis developed here to other, more physical, recurring stochastic processes with nonstationary increments. For example, the amount of daily precipitation recorded at a fixed location [5,26–29] may be amenable to such analysis. If the underlying (stochastic) process is assumed to repeat itself each year, an ensemble can be constructed using the data for each year. Similarly, the daily or monthly abundance of solar flares [5,29–31] may also be amenable to our methods of analysis. Solar activity is known to have an 11-year cycle, so that the days or months at the same phase each cycle may form an ensemble. The approach may also be useful for analyzing hard turbulence [13]; here the temperature variation at a given location may be taken to be a stochastic process with nonstationary increments [5,29]. The process may then be considered to repeat after a nonperiodic triggering event, such as a boundary layer separation [13]. In this case, the temperatures at a given time following the triggering event form an ensemble. In each of these systems, it would be interesting to learn if the scaling is anomalous, and, if so, which of the Noah, Joseph, and Moses effects, or what combination thereof, leads to the anomaly.

ACKNOWLEDGMENTS

This work was supported by NSF-DMR-1507371 (K.E.B.) and NSF-IOS-1546858 (K.E.B.).

[1] F. Black and M. Scholes, J. Polit. Econ. **81**, 637 (1973).
[2] B. Mandelbrot, J. Bus. **36**, 394 (1963).
[3] R. N. Mantegna and H. E. Stanley, Nature (London) **376**, 46 (1995).
[4] L. Le Cam, in *Proceedings of the Fourth Berkeley Symposium on Mathematical Statistics and Probability* (University of California Berkeley, Berkeley, CA, 1961), Vol. 3, pp. 165.
[5] C. W. Richardson, Water Resour. Res. **17**, 182 (1981).
[6] H. Wheater, R. Chandler, C. Onof, V. Isham, E. Bellone, C. Yang, D. Lekkas, G. Lourmas, and M.-L. Segond, Stochast. Environ. Res. Risk Assess. **19**, 403 (2005).
[7] G. Viswanathan, S. V. Buldyrev, S. Havlin, M. Da Luz, E. Raposo, and H. E. Stanley, Nature (London) **401**, 911 (1999).
[8] D. W. Sims, E. J. Southall, N. E. Humphries, G. C. Hays, C. J. Bradshaw, J. W. Pitchford, A. James, M. Z. Ahmed, A. S. Brierley, M. A. Hindell *et al.*, Nature (London) **451**, 1098 (2008).
[9] B. Soibam, L. Chen, G. Roman, and G. Gunaratne, Eur. Phys. J. Spec. Top. **223**, 1787 (2014).
[10] B. Mandelbrot, *Gaussian Self-affinity and Fractals: Globality, The Earth, 1/f Noise, and R/S* (Springer Science & Business Media, New York, 2002), Vol. 8.
[11] P. Embrechts and M. Maejima, *Selfsimilar Processes* (Princeton University Press, Princeton, NJ, 2002).
[12] P. M. Iannaccone and M. K. Khokha, *Fractal Geometry in Biological Systems* (CRC, Boca Raton, FL, 1995).
[13] B. Castaing, G. Gunaratne, F. Heslot, L. Kadanoff, A. Libchaber, S. Thomae, X.-Z. Wu, S. Zaleski, and G. Zanetti, J. Fluid Mech. **204**, 1 (1989).
[14] B. G. Malkiel and E. F. Fama, J. Finance **25**, 383 (1970).
[15] B. G. Malkiel, J. Econ. Perspect. **17**, 59 (2003).
[16] J. Alvarez-Ramirez, J. Alvarez, E. Rodriguez, and G. Fernandez-Anaya, Physica A **387**, 6159 (2008).

[17] C. Eom, S. Choi, G. Oh, and W.-S. Jung, Physica A **387**, 4630 (2008).
[18] Y. Wang and L. Liu, Energy Econ. **32**, 987 (2010).
[19] B. B. Mandelbrot and J. R. Wallis, Water Resour. Res. **4**, 909 (1968).
[20] I. I. Eliazar and M. F. Shlesinger, Phys. Rep. **527**, 101 (2013).
[21] *Genesis 6:1-9:7, The Holy Bible, New King James Version* (Nelson, Nashville, 1982).
[22] *Genesis 41:1-56, The Holy Bible, New King James Version* (Nelson, Nashville, 1982).
[23] K. E. Bassler, J. L. McCauley, and G. H. Gunaratne, Proc. Natl. Acad. Sci. (USA) **104**, 17287 (2007).
[24] U. A. Müller, M. M. Dacorogna, R. B. Olsen, O. V. Pictet, M. Schwarz, and C. Morgenegg, J. Bank. Finance **14**, 1189 (1990).
[25] M. M. Dacorogna, U. A. Müller, R. J. Nagler, R. B. Olsen, and O. V. Pictet, J. Int. Money Finance **12**, 413 (1993).
[26] J. W. Kantelhardt, E. Koscielny-Bunde, D. Rybski, P. Braun, A. Bunde, and S. Havlin, J. Geophys. Res. Atmos. **111**, 1106 (2006).
[27] J. W. Kantelhardt, D. Rybski, S. A. Zschiegner, P. Braun, E. Koscielny-Bunde, V. Livina, S. Havlin, and A. Bunde, Physica A **330**, 240 (2003).
[28] N. Brunsell, J. Hydrol. **385**, 165 (2010).
[29] S. Rehman, Chaos Solitons Fractals **39**, 499 (2009).
[30] F. Lepreti, P. Fanello, F. Zaccaro, and V. Carbone, Sol. Phys. **197**, 149 (2000).
[31] R. Oliver and J. L. Ballester, Phys. Rev. E **58**, 5650 (1998).
[32] *Numbers 33:1-49, The Holy Bible, New King James Version* (Nelson, Nashville, 1982).
[33] J. L. McCauley, K. E. Bassler, and G. H. Gunaratne, Physica A **387**, 202 (2008).
[34] G. H. Gunaratne, J. L. McCauley, M. Nicol, and A. Török, J. Stat. Phys. **121**, 887 (2005).
[35] K. E. Bassler, G. H. Gunaratne, and J. L. McCauley, Physica A **369**, 343 (2006).
[36] J. L. McCauley, G. H. Gunaratne, and K. E. Bassler, Physica A **379**, 1 (2007).
[37] Á. L. Alejandro-Quiñones, K. E. Bassler, M. Field, J. L. McCauley, M. Nicol, I. Timofeyev, A. Török, and G. H. Gunaratne, Physica A **363**, 383 (2006).
[38] J. L. McCauley, *Dynamics of Markets: The New Financial Economics* (Cambridge University Press, Cambridge, 2009).
[39] L. Seemann, J.-C. Hua, J. L. McCauley, and G. H. Gunaratne, Physica A **391**, 6024 (2012).
[40] J.-C. Hua, L. Chen, L. Falcon, J. L. McCauley, and G. H. Gunaratne, Physica A **419**, 221 (2015).
[41] J. L. McCauley, Physica A **387**, 5518 (2008).
[42] J. L. McCauley, K. E. Bassler, and G. H. Gunaratne, Physica A **387**, 3916 (2008).
[43] P. Sibani, Europhys. Lett. **101**, 30004 (2013).
[44] J. P. Bouchaud, J. Phys. I **2**, 1705 (1992).
[45] G. Bel and E. Barkai, Phys. Rev. Lett. **94**, 240602 (2005).
[46] C.-K. Peng, S. V. Buldyrev, S. Havlin, M. Simons, H. E. Stanley, and A. L. Goldberger, Phys. Rev. E **49**, 1685 (1994).
[47] B. B. Mandelbrot and J. R. Wallis, Water Resour. Res. **5**, 967 (1969).
[48] F. Avram and M. S. Taqqu, Statist. Inf. Stochast. Proc. **3**, 69 (2000).
[49] H. E. Hurst, Trans. Am. Soc. Civil Eng. **116**, 770 (1951).
[50] G. Samoradnitsky and M. S. Taqqu, *Stable Non-Gaussian Random Processes: Stochastic Models with Infinite Variance* (CRC, Boca Raton, FL, 1994), Vol. 1.
[51] See Supplemental Material at http://link.aps.org/supplemental/10.1103/PhysRevE.95.042141 for a proof for Eq. (10) and a discussion of the effects on changes in the measurement frequency.
[52] W. Feller, *An Introduction to Probability Theory and Applications* (Wiley, New York, 1957).
[53] B. B. Mandelbrot, Z. Wahrsch. Verwandt. Geb. **31**, 271 (1975).
[54] F. Avram, *Some Limit Theorems for Stationary Sequences with Infinite or Finite Variance* (Cornell University Press, Ithaca, NY, 1986).
[55] M. D. Donsker, Amer. Math. Soc. **6**, 1 (1951).
[56] P. Billingsley, *Convergence of Probability Measures* (Wiley, New York, 2013).
[57] W. Whitt, *Stochastic-process Limits: An Introduction to Stochastic-process Limits and Their Application to Queues* (Springer Science & Business Media, New York, 2002).
[58] P. J. Brockwell and R. A. Davis, *Time Series: Theory and Methods* (Springer Science & Business Media, New York, 2013).
[59] T. Dieker, M.Sc. thesis, University of Twente, Amsterdam, The Netherlands, 2004.
[60] J.-M. Bardet, G. Lang, G. Oppenheim, A. Philippe, and M. S. Taqqu, *Theory and Applications of Long-range Dependence* (Birkhauser, Boston, 2003), p. 579.
[61] R. B. Davies and D. Harte, Biometrika **74**, 95 (1987).
[62] C. Dietrich and G. N. Newsam, SIAM J. Sci. Comput. **18**, 1088 (1997).
[63] A. T. A. Wood and G. Chan, J. Comput. Graph. Stat. **3**, 409 (1994).
[64] B. V. Gnedenko, A. N. Kolmogorov, Am. J. Math. **105**, 28 (1954).
[65] V. V. Uchaikin and V. M. Zolotarev, *Chance and Stability: Stable Distributions and Their Applications* (Walter de Gruyter, Utrecht, 1999).
[66] J. P. Nolan, *Stable Distributions—Models for Heavy Tailed Data* (Birkhauser, Boston, 2015), in progress, Chap. 1 online at academic2.american.edu/∼jpnolan.
[67] J. M. Chambers, C. L. Mallows, and B. Stuck, J. Am. Stat. Assoc. **71**, 340 (1976).
[68] S. Stoev and M. S. Taqqu, Fractals **12**, 95 (2004).
[69] W. B. Wu, G. Michailidis, and D. Zhang, IEEE Trans. Inf. Theor. **50**, 1086 (2004).
[70] D. C. Caccia, D. Percival, M. J. Cannon, G. Raymond, and J. B. Bassingthwaighte, Physica A **246**, 609 (1997).
[71] L. Bisaglia and D. Guégan, Computat. Statist. Data Anal. **27**, 61 (1998).
[72] M. S. Taqqu, V. Teverovsky, and W. Willinger, Fractals **03**, 785 (1995).
[73] K. H. Hamed, Water Resour. Res. **43**, W04413 (2007).
[74] R. Cont, Quantitative Finance **1**, 223 (2001).